# Vibrational Spectroscopy of Ethanol Molecules and Complexes Selectively Prepared in the Gas Phase and Adsorbed on Large Argon Clusters

**Markus Ehbrecht and Friedrich Huisken***

*Max-Planck-Institut für Strömungsforschung, Bunsenstrasse 10, D-37073 Göttingen, Germany*

*Received: June 2, 1997; In Final Form: July 16, 1997*[⊗]

Molecular beam depletion spectroscopy (MBDS) has been employed to study the dissociation of ethanol monomers [$C_2H_5OH$], dimers [$(C_2H_5OH)_2$], and trimers [$(C_2H_5OH)_3$]. In the spectral region between 870 and 1100 $cm^{-1}$, which was accessed with a $CO_2$ laser, four vibrational modes were investigated: the symmetric and asymmetric CCO stretches and the in-plane and out-of-plane rocking modes. Contributions from larger ethanol polymers have been eliminated by dispersing the $(C_2H_5OH)_n$ clusters with a secondary He beam and measuring the laser-induced depletion off-axis in the scattered cluster beam. To study the $C_2H_5OH$ monomer, ethanol molecules were deposited on large $Ar_N$ clusters employing the pickup technique. Ethanol dimers and trimers attached to argon clusters have been studied as well. In a computational approach, the structures of ethanol dimers and trimers have been determined by total energy minimization. These theoretical results are of great value for the interpretation of the experimental data as far as the expected splitting of vibrational bands is concerned. The present investigations allow us to give a consistent interpretation of the available data ranging from the gas phase to the liquid as well as to the bulk matrix.

## Introduction

Small- and medium-sized clusters are recognized as ideal model systems for the study of solvation phenomena on a microscopic level. In this regard hydrogen-bonded systems are of particular relevance in both chemistry and biology. Besides water, the primary alcohols constitute important representatives in this class of molecules. To understand the role of the solvent molecules in a solution, the interaction between the solvent molecules must be understood as well. Therefore, hydrogen-bonded clusters are an active area of current research. As far as the alcohols are concerned, most experimental work has been concentrated on methanol ($CH_3OH$), the simplest alcohol, exciting the C−O stretch[1−5] and the O−H stretch.[6,7]

Up to now only very few studies have been devoted to the IR spectroscopy of ethanol ($C_2H_5OH$) complexes. Two reasons seem responsible for the scarce information available for this system. (1) Ethanol molecules appear as two different conformers which are distinguished by the orientation of the hydroxyl group relative to the methylene group. The two species are designated *trans*- and *gauche*-ethanol. The abundance ratio of the two conformers at room temperature in the gas phase is 6:4 in favor of the *gauche*-conformation.[8] (2) The ethanol molecule is composed of nine atoms and therefore has 21 vibrational modes. As a result, it gives rise to a very complex vibrational spectrum which gets even more complicated if ethanol polymers are involved.

A detailed study on the IR spectroscopy of ethanol and its deuterated variants in the gas phase and in diluted solution as well as in the liquid and solid states has been carried out by Perchard and Josien.[9] In the spectral region between 800 and 1200 $cm^{-1}$ four vibrational modes could be identified: the symmetric and asymmetric CCO stretches, $\nu_s$(CCO) and $\nu_a$-(CCO), and the in-plane and out-of-plane $CH_3$ rocking modes, $r_{||}(CH_3)$ and $r_{\perp}(CH_3)$. Their assignment was complicated due to the strong coupling between the various modes. For example, it was found that the $CH_3$ rocking modes were coupled with the OH bending mode $\delta$(COH).[9] The measurements in solution as well as in the liquid and solid states yielded valuable information on the self-association of ethanol.

The detailed studies of Perchard and Josien[9] have stimulated theoreticians to calculate the infrared vibrational spectra of ethanol and its deuterated isotopomers.[8,10] These theoretical studies revealed that the coupling between the vibrational modes was indeed very strong, particularly in the region between 1000 and 1100 $cm^{-1}$ (ref 8), and that the splitting resulting from the existence of the two conformers was between 4 and 45 $cm^{-1}$ in this spectral range.[10] In both theoretical studies, the force fields were scaled to achieve better agreement with the experiment of Perchard and Josien. Unfortunately, the authors[8,10] did not take the gas phase spectrum as reference; but instead, they fitted their theoretical spectrum to the solution spectrum which has the problem that the absorption lines are considerably broadened and shifted due to the interaction with the solvent molecules. In addition, the solution spectrum may be dominated by ethanol polymers.

Barnes and Hallam[11] studied the spectroscopy of ethanol suspended in argon matrixes at 20 K. Due to the low temperature, the line widths were significantly reduced, giving rise to a rich structure in the spectral region between 1000 and 1100 $cm^{-1}$. Some splittings were traced back to the existence of the two conformers. In addition, Barnes and Hallam proposed different assignments. Thus, the lines near 1030 $cm^{-1}$ were now attributed to $r_{||}(CH_3)$ [$r_{\perp}(CH_3)$ at Perchard and Josien] while the lines between 1050 and 1080 $cm^{-1}$ were assigned to $r_{\perp}$-$(CH_3)$ [$\nu_a$(CCO) at Perchard and Josien]. Finally, the $r_{||}(CH_3)$ band of Perchard and Josien was now attributed to $\nu_a$(CCO). Furthermore, Barnes and Hallam found some weaker features between 1025 and 1060 $cm^{-1}$ which, as a result of their concentration dependence, were assigned to ethanol dimers and larger polymers.

The only IR dissociation experiments of gas-phase ethanol (and ethanol−water) clusters were carried out by Stace and coworkers.[12] They investigated the spectral region between 1042 and 1058 $cm^{-1}$ and observed, with increasing mass of the detected ion, a small red-shift of the absorption maximum at 1055 $cm^{-1}$. Since many cluster sizes contributed to the

[⊗] Abstract published in *Advance ACS Abstracts,* September 1, 1997.

S1089-5639(97)01775-1 CCC: $14.00 

dissociation signal, it was not possible to derive specific information on the absorption behavior of the small ethanol complexes.

In this situation we found it worthwhile to investigate in more detail the spectroscopy of small ethanol polymers in our crossed molecular beam apparatus which makes use of the kinematic size selection technique introduced earlier by Buck and Meyer.[13] This technique is based on the different kinematic behavior of different cluster sizes in a scattering process with rare gas atoms. Choosing the proper deflection angle and mass setting of the mass spectrometer, it is possible to perform size-selective spectroscopy unaffected from fragmentation artifacts of larger polymers. In the past, this molecular beam machine has been successfully employed to study various hydrogen-bonded systems in the 3 and 10 $\mu$m spectral regions. Most notable examples are $(CH_3OH)_n$ (ref 5), $(NH_3)_n$ (ref 14), $(HF)_n$ (ref 15), $(H_2O)_n$ (ref 16), and $(HCOOH)_n$ (ref 17) with $n$ varying from 2 to 4 in most cases. As far as the gas-phase species are concerned, the present study will focus exclusively on the ethanol dimer and trimer.

To obtain complementary spectroscopic information, in particular on the ethanol monomer, we have also studied the spectroscopy of ethanol molecules and small polymers attached to large argon clusters. These systems have been prepared employing the pickup technique introduced by Gough et al.[18] Similar experiments on methanol,[19] methyl fluoride,[20] ammonia,[21] and water[16] adsorbed on argon clusters have proved that such studies provide valuable information elucidating the transition from gas-phase to bulk matrix spectra. Furthermore, it has been shown that this technique provides a unique possibility to study the respective monomeric species at rather low temperature ($T \approx 35$ K)[21] in a molecular beam depletion experiment.

In a computational approach, we have determined the structures of ethanol dimers and trimers by minimizing their total energies and taking into account the existence of one *trans*-geometry and two *gauche*-geometries. For the ethanol dimer only open-chain structures with nonequivalent constituents (proton donor and acceptor) were found, whereas for the trimer, the minimum-energy configurations were always cyclic. These structure calculations are used to deduce valuable information on the splittings of vibrational bands.

## Experimental Section

The experiments have been carried out in a crossed molecular beam machine which has been described elsewhere.[22] Detailed experimental information relevant to the present work may be found in the publications devoted to the study of size-selected gas-phase methanol complexes[5] and methanol complexes attached to argon clusters.[19] The $(C_2H_5OH)_n$ cluster beam was generated by bubbling neon at a total pressure of 1 bar through a reservoir of spectroscopic grade ethanol (Merck, Darmstadt) kept at a temperature of $-9.4$ °C. These conditions have been determined by optimizing the signal of the scattered ethanol dimers with the detector positioned to a deflection angle of $\Theta = 10°$ (see below). The resulting mixture of 0.8% ethanol in Ne was expanded through a 0.1 mm diameter thin-walled nozzle kept at room temperature. The beam was collimated by a 0.4 mm diameter skimmer and transferred to a differential chamber where it was crossed by the radiation of a pulsed $CO_2$ laser. After a second collimator of 2 mm diameter, the ethanol cluster beam was dispersed by scattering it from a secondary helium beam. Finally, the selected cluster species were detected off-axis by a rotatable mass spectrometer detector equipped with electron impact ionizer ($I = 15$ mA, $E = 100$ eV), quadrupole mass spectrometer, and open electron multiplier. Spectra of undispersed cluster beams were measured with a 0.2 mm diameter pinhole in front of the detector entrance. All relevant beam parameters are collected in Table 1.

**TABLE 1: Molecular Beam Parameters**

| | primary beam | secondary beam |
|---|---|---|
| species | 0.8% $C_2H_5OH$ in Ne | He |
| bath temp/K | 263.8 | |
| source temp/K | 299 | 299 |
| stagnation press./bar | 1 | 25 |
| nozzle diameter/mm | 0.1 | 0.03 |
| skimmer diameter/mm | 0.4 | 0.4 |
| most probable velocity/m $s^{-1}$ | 781 | 1763 |

Ethanol complexes attached to large argon clusters $[(C_2H_5OH)_n \cdot Ar_N]$ have been generated by employing the pickup technique introduced by Gough et al.[18] The corresponding setup is described in more detail in our publications devoted to methanol[19] and ammonia[21] molecules and complexes adsorbed on argon host clusters. Briefly, argon clusters ($Ar_N$) with an estimated mean size of $\langle N \rangle = 70$ were produced by expanding argon gas at a pressure of $p_0 = 7$ bar through a 50 $\mu$m diameter thin-walled nozzle. Before entering the differential chamber through the skimmer, the argon cluster beam was crossed by a beam of ethanol molecules emanating from an effusive molecular beam source operated at stagnation pressures between 10 and 50 mbar. Upon the collisions, monomeric ethanol molecules were attached to the argon clusters and carried by them to the detector. At larger ethanol pressures multiple adsorption occurred, and by interacting through their large dipole moment, the ethanol molecules aggregated and formed small polymers within or on the surface of the host clusters. Due to the strong fragmentation of the composite clusters in the ionizer, the small ethanol complexes could be detected on the typical fragmentation channels known from gas-phase mass spectrometry of free ethanol polymers.

As laser source, a line-tunable pulsed $CO_2$ laser (Lambda Physik, model EMG 201) was used. The laser beam was focused by a cylindrical ZnSe lens producing a 25 mm wide and 4 mm high rectangular beam profile at the position where it intersected the cluster beam, which was 2 mm high. The laser was line-tuned through the 9$\mu$P and 9$\mu$R branches, thus covering the spectral region between 1020 and 1090 $cm^{-1}$ with a small gap at 1063 $cm^{-1}$. Using the $^{13}CO_2$ isotope, it was possible to access the spectral range between 870 and 910 $cm^{-1}$ and to study the symmetric CCO stretch. The absorption spectra of ethanol dimers and trimers were recorded by measuring the laser-induced depletion as a function of frequency for different deflection angles and mass settings of the quadrupole, whereas the spectra of ethanol molecules and polymers adsorbed on argon clusters were determined in the undispersed beam without size selection.

## Results

**Mass Spectrometry.** Although conventional mass spectra of $(C_2H_5OH)_n$ cluster beams are of limited value because of the expected strong fragmentation upon ionization, they provide an estimate of the lower limit of the maximum cluster size present in the beam and give information on possible fragmentation channels. Therefore, we have measured mass spectra in the direct undispersed cluster beam. The mass spectrum, recorded with background subtraction under the conditions employed later for the dissociation experiments (see Table 1), is shown in Figure 1. Except for the carrier gas peaks at $m =$ 10 [$^{20}Ne^{2+}$], 11 [$^{22}Ne^{2+}$], 20 [$^{20}Ne^{+}$], and 22 amu [$^{22}Ne^{+}$] and a group of peaks around $m = 31$ amu [$CH_3O^{+}$], which are due

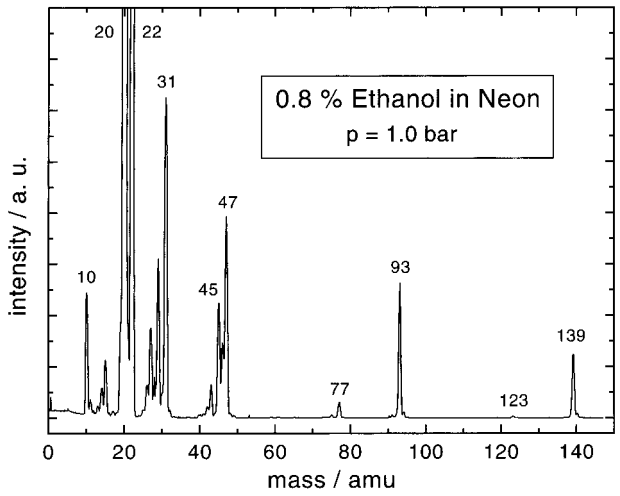


**Figure 1.** Mass spectrum of the ethanol cluster beam produced by expanding 0.8% ethanol in neon at a stagnation pressure 1 bar.

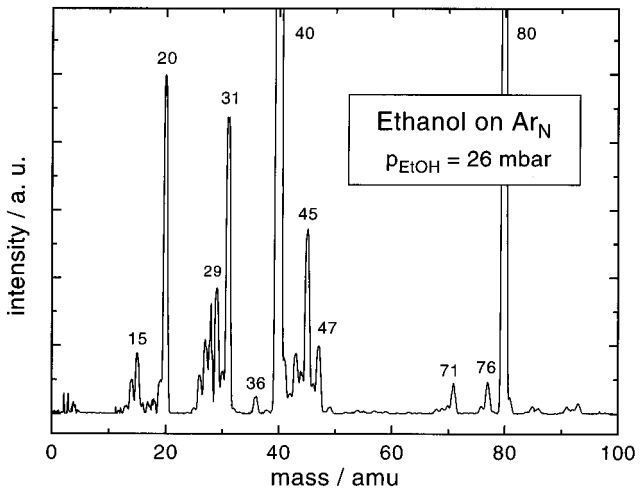


**Figure 2.** Mass spectrum of argon clusters doped with ethanol molecules. The argon gas was expanded at a pressure of 7 bar while the ethanol source was operated with 26 mbar. Note that almost all mass peaks correspond to fragments of the ionized $(C_2H_5OH)_n{\cdot}Ar_N$ clusters.

to fragments of ethanol molecules and clusters, some stronger lines were observed at $m = 45$ [$CH_3CH_2O^+$], 47 [$(CH_3CH_2OH)H^+$], 93 [$(CH_3CH_2OH)_2H^+$], and 139 amu [$(CH_3CH_2OH)_3H^+$].

Due to an intracluster ion−molecule reaction

$$(CH_3CH_2OH)_n^+ \rightarrow (CH_3CH_2OH)_{n-1}H^+ + CH_3CH_2O^\bullet \quad (1)$$

which proceeds rapidly within the ionized $(CH_3CH_2OH)_n$ cluster, ethanol clusters are predominantly detected as protonated $(n - 1)$ clusters.[23] Reaction (1) is also observed for other hydrogen-bonded complexes and in particular for methanol clusters.[5] In case of methanol complexes, it was found that the protonated $(n - 1)$ clusters further fragment by evaporating one or more monomer units.[24] The smaller peaks at $m = 77$ and 123 amu can be attributed to ionized ethanol dimers and trimers having lost a methyl group (i.e., to $(CH_3CH_2OH)CH_2OH^+$ and $(CH_3CH_2OH)_2CH_2OH^+$, respectively). As we will show later, the contribution of larger clusters to these fragment masses is very small. From the mass spectrum shown in Figure 1, it is rather obvious that the mass settings $m = 45$ [$CH_3CH_2O^+$], 47 [$(CH_3CH_2OH)H^+$], and 93 amu [$(CH_3CH_2OH)_2H^+$] seem most favorable to detect gas-phase ethanol molecules, dimers, and trimers, respectively. But care must be taken since all signals may be affected by fragmenting larger ethanol clusters if they are present in the beam.

A mass spectrum measured for argon clusters doped with ethanol molecules using the pickup technique is shown in Figure 2. For this experiment the stagnation pressure in the argon cluster source was $p_0 = 7$ bar while the pressure in the effusive ethanol source was chosen to be $p_0 = 26$ mbar. Naturally, the most prominent peaks in the mass spectrum at $m = 20$, 40, and 80 amu are due to fragments of the argon host clusters. In contrast, the groups of peaks around $m = 15$ ($CH_3^+$), 31 ($CH_3O^+$), and 45 amu ($C_2H_5O^+$) are assigned to fragments of ethanol guest molecules carried by the host clusters to the detector. Note that the fragmentation patterns are very similar to those encountered for gas-phase ethanol molecules (see Figure 1). The peak at $m = 47$ amu [$(C_2H_5OH)H^+$] indicates that two ethanol molecules have been absorbed by the argon host clusters. They have interacted through their dipole moment, thus forming a dimer which, according to reaction (1), can be detected at mass $m = 47$ amu.

Some of the groups just discussed reappear with reduced intensity at a position shifted by 40 amu to higher masses. Therefore, they must be assigned to ethanol fragments complexed with one argon atom. For example, the peaks at $m = 71$ and 85 amu are due to $Ar{\cdot}CH_3O^+$ and $Ar{\cdot}C_2H_5O^+$, respectively. It is interesting to note that the peak at $m = 86$ amu corresponds to the unprotonated complex of ethanol and argon ($Ar{\cdot}C_2H_5OH^+$). As has been shown earlier for $CH_3F$ and $CH_3OH$,[25] the argon host cluster may provide a suitable environment to quench the protonation reaction (1). As for gas-phase ethanol clusters, the $(C_2H_5OH)CH_3O^+$ ion is observed at $m = 77$ amu. The protonated ethanol dimer [$(C_2H_5OH)_2H^+$] appearing at $m = 93$ amu most probably originates from the ethanol trimer.

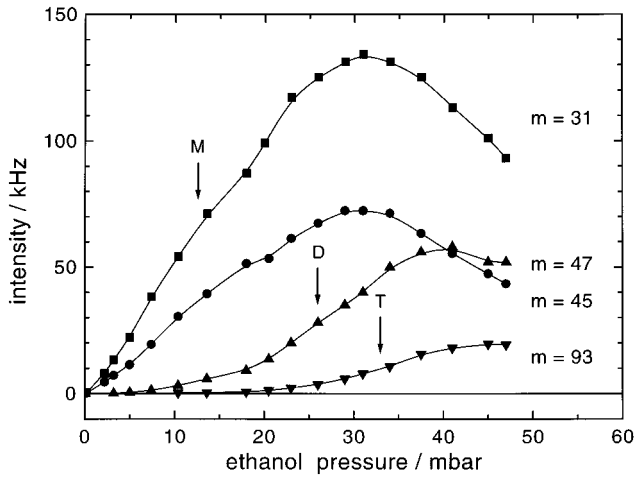


**Figure 3.** Count rates measured on selected masses as a function of the pressure in the effusive ethanol source. The arrows indicate the conditions employed for measuring dissociation spectra of ethanol monomers (M), dimers (D), and trimers (T) attached to large argon clusters.

The mass spectrum shown in Figure 2 enables us to select the most favorable masses for detecting ethanol complexes attached to argon host clusters. These are for the monomer $m = 31$ amu, for the dimer $m = 47$ amu, and for the trimer $m = 93$ amu. In the following we have measured the signals on these masses as a function of the ethanol source pressure. The respective dependencies are shown in Figure 3. The behavior of the two curves measured at $m = 31$ and $m = 45$ amu is very similar. At small pressure values they rise rather linearly, as is expected for a monomer signal, and at values larger than 30 mbar the two curves decrease again. This decrease is due to

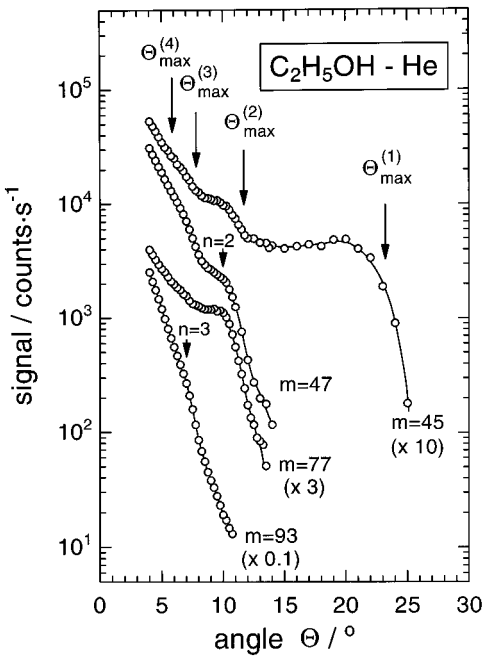


**Figure 4.** Angular distributions of gas phase ethanol clusters scattered from a helium secondary beam. The arrows above the $m = 45$ curve denote the maximum scattering angles $\Theta^{(n)}_{max}$ for the various cluster sizes $n$ as expected from the Newton diagram. The arrows labeled with $n = 2$ and $n = 3$ indicate the detector settings used for measuring the dimer and trimer dissociation spectra, respectively.

an enhanced formation of ethanol complexes as is evidenced by the curves measured at $m = 47$ and 93 amu which reflect the formation of dimers and trimers, respectively. As we know from our experiments on methanol complexes attached to argon clusters,[19] fragmentation of the ionized ethanol complexes is somewhat reduced because of the moderating argon environment, but it may still be a serious problem. Therefore, it is recommended to choose, for each cluster size, the conditions as moderate as possible. To work at sufficiently high signal levels, we have selected the ethanol pressures marked by arrows to study the spectroscopy of monomers (M), dimers (D), and trimers (T) attached to argon host clusters.

**Size Selection.** To select the gas-phase ethanol clusters according to their size, we employ the kinematic size selection of a scattering experiment. This technique was introduced by Buck and Meyer[13] and makes use of the fact that lighter clusters are scattered into a larger angular range than the heavier species which are confined to smaller angles. The maximum scattering angles for each cluster size are derived from the so-called Newton diagram.[22] For the conditions employed in the present experiment (see Table 1), the following maximum deflection angles are calculated assuming purely elastic scattering: $\Theta^{(1)}_{max} = 23.2°$, $\Theta^{(2)}_{max} = 11.7°$, $\Theta^{(3)}_{max} = 7.8°$, and $\Theta^{(4)}_{max} = 5.9°$.

We have measured angular distributions of ethanol monomers and clusters for various mass settings of the quadrupole mass spectrometer. The curves measured at the most prominent masses $m = 45$ [$CH_3CH_2O^+$], 47 [$(CH_3CH_2OH)H^+$], and 93 amu [$(CH_3CH_2OH)_2H^+$] are plotted in Figure 4. In addition, we have included the angular distribution measured with the mass spectrometer tuned to $m = 77$ amu [$(CH_3CH_2OH)CH_2OH^+$]. Note that the $y$-axis numbering applies only to the $m = 47$ curve and that the other curves are shifted as indicated in the figure to provide a better comparison. The arrows designated with $\Theta^{(n)}_{max}$ indicate the maximum scattering angles for the respective $(C_2H_5OH)_n$ cluster sizes with $n = 1-4$ while the short arrows labeled with $n = 2$ and $n = 3$ mark the positions chosen for the size-selective experiments (see below).

Mass $m = 45$ amu [$C_2H_5O^+$] constitutes the most important monomer fragmentation channel. Correspondingly, the signal on mass $m = 45$ amu can be observed up to (and slightly beyond) the maximum monomer scattering angle $\Theta^{(1)}_{max} = 23.2°$. Just below $\Theta^{(2)}_{max} = 11.7°$ the $m = 45$ curve exhibits a pronounced shoulder which is generated by ethanol dimers fragmenting to $C_2H_5O^+$. Note that, around $\Theta = 10°$, the dimer contribution to the signal on $m = 45$ amu is practically the same as the monomer contribution. If the detector is further moved to smaller angles another shoulder is observed just below $\Theta^{(3)}_{max} = 7.8°$. This shoulder is now due to ethanol trimers fragmenting into $C_2H_5O^+$ ions as well. We would like to mention that the angular distribution measured on $m = 43$ amu [$C_2H_3O^+$], which is not shown in the figure, features the same dimer shoulder as the $m = 45$ curve, indicating that the dimer fragmentation to this mass is also very pronounced. In contrast, the dimer contribution to the signal on the monomer parent mass, $m = 46$ amu, was found to be very weak.

The angular distribution denoted by $m = 47$ has been measured with the mass spectrometer tuned to $(C_2H_5OH)H^+$, the typical dimer fragmentation channel. As expected, it shows a pronounced dimer shoulder near $\Theta^{(2)}_{max}$. In addition, another slightly less pronounced shoulder is clearly visible below $\Theta^{(3)}_{max}$. This contribution is attributed to ethanol trimers which, after being ionized, undergo the ion−molecule reaction 1 and evaporate a monomer unit to yield $(C_2H_5OH)H^+$. When the mass spectrometer is tuned to $m = 93$ amu, a significant increase in signal occurs near $\Theta^{(3)}_{max}$. Just below this angle exclusively trimers are observed at $m = 93$ amu.

The measured angular distributions confirm that the ionization-induced fragmentation of the various ethanol clusters into smaller species is very pronounced. They further demonstrate that it is possible to achieve complete size selection. For example, if the detector is moved to the deflection angle denoted by $n = 2$ and the mass spectrometer tuned to $m = 47$ amu, exclusively ethanol dimers will be detected. Similarly, at $m = 93$ amu and the position labeled with $n = 3$, ethanol trimers may be studied, essentially unaffected by larger clusters.

A final remark should be devoted to the angular distribution measured at mass $m = 77$ amu, which corresponds to the ion obtained from the ionized ethanol dimer [$(C_2H_5OH)_2^+$] after abstraction of the methyl group. Comparing this curve with the $m = 47$ data, it is clearly seen that the fragmentation of larger ethanol clusters into this channel is considerably reduced. Therefore, this channel would be much more favorable for studying ethanol dimers if size selection were not available. The same conclusion has been drawn by Mori and Kitagawa[23] from their mass spectrometric study of ethanol clusters as a function of source conditions.

## Dissociation Experiments

**Free Gas-Phase Ethanol Complexes.** As we have just discussed, it is possible to study the ethanol dimer, unaffected from larger clusters, when the detector is positioned to $\Theta = 10°$ (position $n = 2$ in Figure 4) while the mass spectrometer is tuned to $m = 47$ amu. We have searched for dimer dissociation near 1054 $cm^{-1}$ where Stace and co-workers[12] observed an absorption band with the mass spectrometer tuned to $(C_2H_5OH)_2H^+$. We found maximum dissociation at the 9$\mu$P(6) $CO_2$ laser line (1058.9 $cm^{-1}$) and measured at first a fluence dependence of the depletion signal. The measured dissociated fraction increased linearly up to a value of 0.55 at a laser fluence of 150 $mJ/cm^2$ and slowly went into saturation beyond this

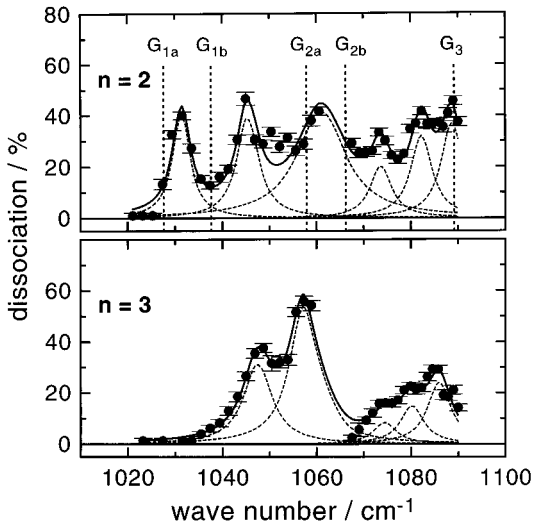


**Figure 5.** Dissociation spectra of gas-phase ethanol dimers ($n = 2$) and trimers ($n = 3$) measured with size selection. The dashed sticks labeled with $G_{1a}$, $G_{1b}$, $G_{2a}$, $G_{2b}$, and $G_3$ denote the Q-branch positions observed in the gas phase by Perchard and Josien.[9]

**TABLE 2: Parameters of the Lorentzian Line Shape Functions Fitted to the Gas-Phase Ethanol Dimer and Trimer Spectra of Figure 5**

| species | band position/cm$^{-1}$ | fwhm/cm$^{-1}$ | dissociated fraction |
|---|---|---|---|
| $n = 2$ | 1031.4 | 4.6 | 0.38 |
| | 1045.4 | 5.6 | 0.41 |
| | 1061.0 | 12.5 | 0.42 |
| | 1073.7 | 5.5 | 0.21 |
| | 1082.3 | 5.5 | 0.31 |
| | 1088.7 | 5.6 | 0.39 |
| $n = 3$ | 1047.5 | 7.3 | 0.31 |
| | 1057.2 | 7.3 | 0.52 |
| | 1074.5 | 6.0 | 0.09 |
| | 1080.2 | 6.0 | 0.15 |
| | 1086.0 | 6.0 | 0.25 |

value. Due to this behavior, we decided to choose the constant fluence of 120 mJ/cm$^2$ for all dissociation experiments presented here.

The upper panel of Figure 5 shows the absorption−dissociation spectrum that we have measured for size-selected ethanol dimers. The integration time for each measuring point was 60 min. Dissociation was observed in the entire region, giving rise to a rather complex spectrum. It reveals at least six absorption bands whose exact positions have been determined by fitting Lorentzian line shape functions to the experimental data. The parameters are collected in Table 2. In the left part of the spectrum, the agreement between experiment and fit is rather good. The same is true for the high-frequency part. However, in the central part of the spectrum, near 1050 cm$^{-1}$ where seven data points have roughly the same height, the simulation deviates from the measurement. Unfortunately, due to the gap between 1060.6 and 1067.5 cm$^{-1}$, it is not possible to determine the exact maximum position and width of the absorption band located near 1061 cm$^{-1}$. Moreover, the limited tuning range of the $CO_2$ laser does not allow us to employ laser frequencies larger than 1090 cm$^{-1}$ so that we cannot decide whether there are additional absorption bands beyond 1090 cm$^{-1}$ or not.

The dashed lines indicate the positions where the absorption bands for gas-phase ethanol molecules were observed.[9] Their positions and assignments are given in Table 3. The complicated structure of the dimer spectrum obviously reflects the fact that the various bands split into two (or perhaps more) components due to the existence of the two nonequivalent monomer units (proton acceptor and donor) in the hydrogen-bonded ethanol dimer. Thus, for example, one is tempted to assign the two bands at 1031.4 and 1045.4 cm$^{-1}$ to the excitation of the methyl rocking vibration in the proton acceptor and donor molecule of the ethanol dimer. A similar splitting has been found for the CO stretching vibration of the methanol dimer.[1,5]

Moving the detector to $\Theta = 7°$ and tuning the mass spectrometer to $m = 93$ amu, we are in a position to measure a pure trimer spectrum. The result is shown in the lower panel of Figure 5. Due to the rather low trimer count rate of 2.7 kHz, the integration time was again chosen to be 60 min. In contrast to the ethanol dimer, the trimer spectrum looks somewhat simpler. This can be easily understood if one assumes that the ethanol trimer has a cyclic structure as is also found for the methanol trimer. In this case the ethanol molecules adopt rather equivalent positions, thus reducing the large splittings observed for the dimer. The left part of the trimer spectrum (below 1060 cm$^{-1}$) can very well be represented by two Lorentzians. Beyond the gap in the laser tuning range, the dissociation is almost zero. Therefore, another absorption band in this narrow range seems very unlikely. At higher frequencies, the dissociation shows a stepwise rise which can be reproduced by three Lorentzians, quite similar to the dimer case.

A complete assignment of the various features observed for the ethanol dimer and trimer seems very difficult. Therefore, we have decided to study the spectroscopy of small ethanol complexes attached to argon clusters. These measurements will supply additional information: (1) it will be possible to locate the ethanol monomer absorptions, and (2) we will be able to compare the spectra with the results obtained in cryogenic argon matrixes, thus leading over from the free gas phase to the bulk matrix.

**Ethanol Complexes Attached to Large Argon Clusters.** If one employs the IR vibrational predissociation technique to investigate the absorption behavior of loosely bound complexes, it is not possible to study the monomer since it does not dissociate upon irradiation with IR photons. However, if this monomer is embedded in or attached to a rare gas cluster and if it is vibrationally excited, the excitation energy is dissipated over the entire cluster, and as a result, several rare gas atoms are evaporated, giving rise to a depletion signal. It has been discussed earlier[26] that this depletion signal mainly results from the reduction of the ionization cross section. Hence, with this technique it will be possible to study the ethanol monomer and to obtain useful information for the interpretation of the ethanol dimer and trimer spectra presented before.

Employing the ethanol pressures and mass spectrometer settings marked by arrows in Figure 3, we have studied the

**TABLE 3: Ethanol Monomer Absorptions Observed between 1000 and 1100 cm$^{-1}$ in the Gas-Phase and Argon Matrix**

| present band designation | gas phase (ref 9) | | | argon matrix (ref 11) | | |
|---|---|---|---|---|---|---|
| | line | position/cm$^{-1}$ | assignt | line | position/cm$^{-1}$ | assignt |
| $\nu_\alpha$ | $G_{1a}$ | 1027.6 | $r_\perp$ ($CH_3$) | $M_{1a}$ | 1016.5 | $r_\parallel$ ($CH_3$) 2nd site |
| | $G_{1b}$ | 1037.6 | | $M_{1b}$ | 1025.0 | $r_\parallel$ ($CH_3$) |
| $\nu_\beta$ | $G_{2a}$ | 1057.9 | $\nu_a$(CCO) | $M_{2a}$ | 1076.6 | $r_\perp$ ($CH_3$) *gauche* |
| | $G_{2b}$ | 1066.2 | | $M_{2b}$ | 1083.2 | $r_\perp$ ($CH_3$) *trans* |
| $\nu_\gamma$ | $G_3$ | 1089.2 | $r_\parallel$ ($CH_3$) | $M_3$ | 1091.7 | $\nu_a$(CCO) |

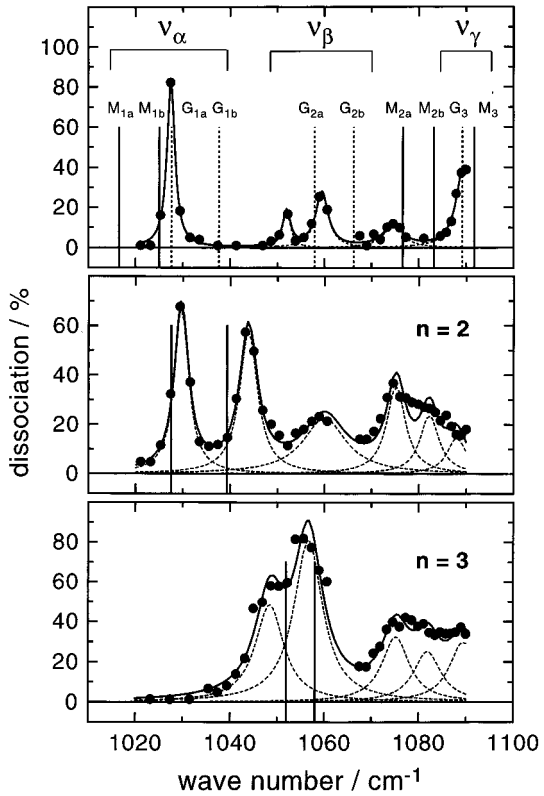


**Figure 6.** Depletion spectra measured for ethanol molecules ($n = 1$), dimers ($n = 2$), and trimers ($n = 3$) adsorbed on large argon clusters. The dashed sticks denote again the Q-branch positions observed in the gas phase,[9] while the solid sticks mark the positions of monomer, dimer, and polymer absorptions recorded by Barnes and Hallam[11] in a cryogenic argon matrix.

**TABLE 4: Parameters of the Lorentzian Line Shape Functions Fitted to the Cluster-Adsorbed Ethanol Spectra of Figure 6**

| species | band position/cm$^{-1}$ | fwhm/cm$^{-1}$ | dissociated fraction |
|---|---|---|---|
| $n = 1$ | 1027.5 | 2.0 | 0.81 |
| | 1052.0 | 2.0 | 0.18 |
| | 1059.4 | 3.2 | 0.27 |
| | 1074.6 | 4.9 | 0.11 |
| | 1089.5 | 3.8 | 0.40 |
| $n = 2$ | 1029.7 | 3.6 | 0.67 |
| | 1043.9 | 4.6 | 0.57 |
| | 1060.0 | 11.0 | 0.23 |
| | 1075.2 | 4.9 | 0.33 |
| | 1082.3 | 4.8 | 0.23 |
| | 1088.0 | 4.9 | 0.14 |
| $n = 3$ | 1048.4 | 7.3 | 0.48 |
| | 1056.7 | 7.4 | 0.81 |
| | 1075.2 | 7.0 | 0.32 |
| | 1081.9 | 7.0 | 0.25 |
| | 1089.5 | 7.0 | 0.29 |

spectroscopy of ethanol monomers, dimers, and trimers attached to argon clusters. The results, which were obtained with an integration time of 15 min per measuring point, are displayed in Figure 6. The ethanol monomer spectrum ($n = 1$) reveals five absorption maxima which have been fitted by Lorentzian line shape functions. The respective parameters are collected in Table 4. The dashed lines (denoted $G_{1a}$, $G_{1b}$, $G_{2a}$, $G_{2b}$, and $G_3$) mark again the positions of the absorption bands observed for gas-phase ethanol molecules.[9] On the other hand, the solid lines (labeled with $M_{1a}$, $M_{1b}$, $M_{2a}$, $M_{2b}$, and $M_3$) indicate the positions where the respective absorptions were located in the argon matrix[11] (see Table 3). It has already been mentioned in the Introduction that the assignments to vibrational modes in the matrix study[11] differ from those made for the gas phase.[9] To avoid confusion and facilitate the further discussion, we will designate the three bands in the order of increasing frequency $\nu_\alpha$, $\nu_\beta$, and $\nu_\gamma$, as indicated in Table 3.

The $\nu_\alpha$ mode of the ethanol molecule attached to an $Ar_N$ cluster, which appears at 1027.3 cm$^{-1}$, coincides almost exactly with the gas-phase Q-branch $G_{1a}$ at 1027.6 cm$^{-1}$ while it is slightly blue-shifted from the band position in the matrix (1025 cm$^{-1}$). However, it is also possible (and even more likely) that the peak of the present study corresponds to the $G_{1b}$ gas-phase line and that the peak corresponding to $G_{1a}$ is located outside the tuning range of the $CO_2$ laser. In this case the observed red-shift would be 10.3 cm$^{-1}$.

The splitting of the $\nu_\beta$ mode, which is observed in the gas phase to be 8.3 cm$^{-1}$ (1066.2−1057.9 cm$^{-1}$), is also present for ethanol attached to argon clusters (1059.5 − 1051.9 = 7.6 cm$^{-1}$). As for the $\nu_\alpha$ vibration, the peaks are red-shifted from the respective gas-phase lines. In the argon matrix, however, this doublet ($M_{2a}$ and $M_{2b}$) appears at a position considerably blue-shifted from the gas-phase values. Barnes and Hallam[11] attribute the splitting to the existence of the two conformers, *gauche*- and *trans*-ethanol. At the high-frequency end of the spectrum, a third band is observed which we designated as $\nu_\gamma$. Its position is very close to both the gas-phase and matrix positions. Unfortunately, the limited tuning range of the $CO_2$ laser prevents us from gaining any information about the higher frequency range. The smaller absorption band found at 1074.7 cm$^{-1}$ has no counterpart, neither in the gas-phase spectrum of Perchard and Josien[9] nor in the matrix study of Barnes and Hallam.[11]

The middle panel of Figure 6 shows the absorption spectrum of ethanol dimers ($n = 2$) attached to argon clusters. It features two pronounced peaks in the region of the $\nu_\alpha$ vibration: a single broad band near 1060 cm$^{-1}$ and a complicated structure at the high-frequency end of the spectrum. Comparing with the gas-phase dimer spectrum displayed in Figure 5, it is stated that the two spectra are very similar. The solid lines at 1027.5 and 1039.3 cm$^{-1}$ denote the dimer positions observed in the argon matrix.[11] Unfortunately, in the matrix study, the lower frequency dimer line overlaps with the $M_{1b}$ monomer line. As for the $\nu_\alpha$ monomer line, we have the result that the dimer frequencies observed in the argon matrix are further shifted to the red than those measured for $(C_2H_5OH)_2$ adsorbed on argon clusters.

The bottom spectrum displayed in Figure 6 has been measured for $(C_2H_5OH)_3$ attached to argon clusters. It features two strong bands at 1048.4 and 1056.7 cm$^{-1}$ and some broad absorption around 1080 cm$^{-1}$. As was already found for the dimer, the spectra of free and cluster-adsorbed trimers are again very similar. The solid lines mark the two positions where absorption bands of ethanol polymers of unspecified size have been observed in the argon matrix.[11]

The gas-phase study of Perchard and Josien[9] locates the next strong absorption band below 1000 cm$^{-1}$ near 880 cm$^{-1}$. It is assigned to the symmetric CCO stretch, $\nu_s$(CCO). This spectral range can be accessed with the $CO_2$ laser if it is operated with the $^{13}CO_2$ isotope. In the final stage of our study, while carrying out the experiments on ethanol attached to argon clusters, we had the opportunity to employ such laser gas and to investigate the symmetric CCO stretch as well. The results are displayed in Figure 7 while the fit parameters are summarized in Table 5. The uppermost spectrum, which has been measured for the ethanol monomer adsorbed on argon clusters, reveals a stronger band at 890.4 cm$^{-1}$ and a much weaker absorption at 878.4 cm$^{-1}$. In their gas-phase study, Perchard and Josien[9] observed three Q-branches whose positions are marked in Figure 7 by

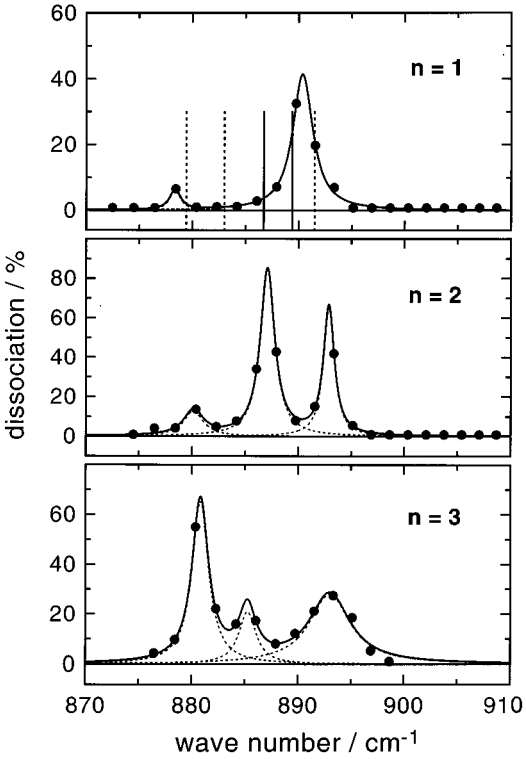


**Figure 7.** Depletion spectra of argon clusters doped with ethanol molecules in the spectral region of the symmetric COO stretch. Dashed and solid sticks mark again the positions of gas phase and matrix bands, respectively.

**TABLE 5: Parameters of the Lorentzian Line Shape Functions Fitted to the Spectra of the Symmetric CCO Stretch Shown in Figure 7**

| species | band position/cm$^{-1}$ | fwhm/cm$^{-1}$ | dissociated fraction |
|---|---|---|---|
| $n = 1$ | 878.4 | 1.2 | 0.06 |
| | 890.4 | 2.3 | 0.41 |
| $n = 2$ | 880.1 | 2.2 | 0.14 |
| | 887.1 | 1.6 | 0.84 |
| | 892.9 | 1.2 | 0.65 |
| $n = 3$ | 880.8 | 1.9 | 0.65 |
| | 885.3 | 1.9 | 0.21 |
| | 893.0 | 4.6 | 0.28 |

the dashed lines. From these three gas-phase lines the highest frequency Q-branch at 891.5 cm$^{-1}$ was the most prominent one. The matrix study of Barnes and Hallam[11] revealed an intense doublet, indicated in Figure 7 by the solid lines, and two weak satellite peaks on either side (near 875 and 895 cm$^{-1}$).

The middle spectrum of Figure 7 shows the result obtained for the ethanol dimer adsorbed on argon clusters. It reveals a splitting of the band which seems to correspond to the strongest monomer band and a weak transition at 880.1 cm$^{-1}$. The trimer spectrum shown in the bottom panel of Figure 7 reveals a complicated structure. Here the lowest frequency band at 880.8 cm$^{-1}$ has become the most prominent feature while the highest frequency band at 893.0 cm$^{-1}$ is now significantly broader.

## Calculations

To facilitate the interpretation of the experimental data, we have carried out calculations to determine the structures of small ethanol clusters, $(C_2H_5OH)_n$ with $n = 2, 3$. The computer program, which has been developed by Schmidt,[27] determines the minimum-energy configurations starting from random geometries and employing the downhill simplex method.[28] Our present calculations are based on the experimentally derived $C_2H_5OH$ monomer geometry given by Alagona and Tani[29] and

**TABLE 6: Potential Energies of Optimized Ethanol Dimer and Trimer Geometries in kJ/mol[a]**

| ethanol dimer | | ethanol trimer | |
|---|---|---|---|
| tr−g1 | −32.84 | 3tr | −83.70 |
| tr−g2 | −32.84 | 2tr−g1 | −81.45 |
| tr−tr | −32.60 | 2tr−g2 | −81.34 |
| g1−g1 | −28.34 | tr−2g1 | −79.05 |
| g2−g2 | −28.34 | tr−2g2 | −79.06 |
| g1−g2 | −28.15 | 3g1 | −76.64 |
| | | 3g2 | −76.65 |
| | | g1−2g2 | −75.94 |
| | | 2g1−g2 | −75.93 |

[a] g1 and g2 denote the two *gauche*-configurations while tr stands for the *trans*-conformer.

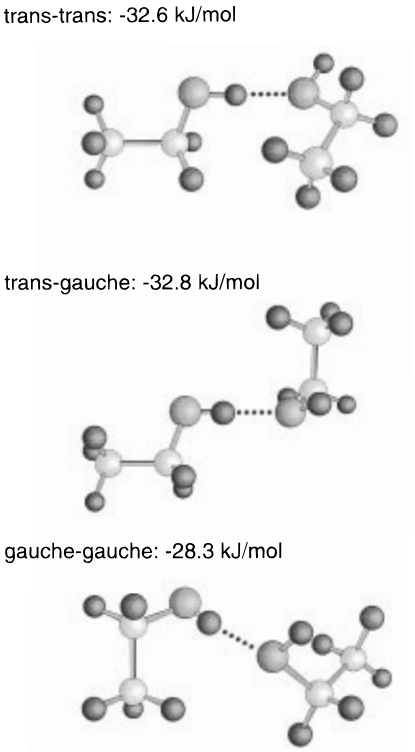


**Figure 8.** Minimum potential energy configurations of ethanol dimers determined for three different conformer combinations.

on the intermolecular pair potential of Jorgensen.[30] This potential has been developed for molecular dynamics calculations to simulate liquid ethanol.

For the ethanol dimer we found an open chainlike minimum-energy configuration with the OH group of one ethanol molecule (proton donor) being engaged in a hydrogen bond with a lone pair orbital of the other ethanol molecule (proton acceptor). The situation is practically the same as for the methanol dimer for which a similar structure was found.[27,31] Due to the existence of two *gauche*-conformers (g1 and g2) and one *trans*-conformer (tr), there are six possibilities to choose the two dimer constituents. The minimum energies of these six dimers are listed in Table 6. Our calculations reveal that the dimers containing the *trans*-ethanol molecule (as proton donor) are more stable by approximately 4 kJ/mol than those being built from two *gauche*-conformers. The geometries of three selected dimer configurations are depicted in Figure 8.

For the ethanol trimer we have determined a cyclic structure with the three O−H bonds arranged in a triangle. The geometries of the two lowest energy configurations are shown in Figure 9. Note that in this configuration each ethanol molecule plays simultaneously the role of a proton acceptor *and* donor. Similar triangular structures have been obtained for the

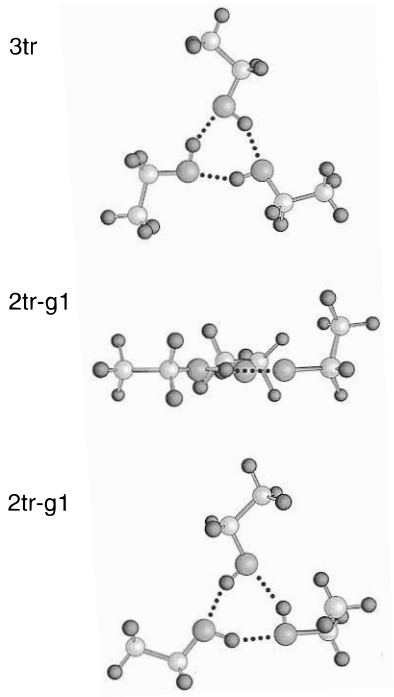


**Figure 9.** Minimum energy structures of two possible ethanol trimers. The trimer consisting of two *trans*-conformers and one *gauche*-conformer is shown in two different views.

water[32−35] and methanol trimer[36] for which high-level ab initio calculations have been carried out. As in the dimer case, the involvement of *trans*-molecules leads to more stable structures. The program was not able to calculate the trimer being built from three different conformers (g1, g2, and tr), but we expect that the binding energy of this species is also near 79 kJ/mol.

Neglecting for a moment the existence of different conformers, we may summarize the structure calculations as follows. The ethanol dimer consists of two nonequivalent molecules that can be characterized as proton acceptor and proton donor. In the ethanol trimer the three molecules adopt rather equivalent positions with each molecule playing the role of a proton acceptor *and* donor. As a result, we expect for the dimer that each vibrational monomer band splits into two components, one being due to the excitation of the proton acceptor while the other is attributed to the proton donor. In contrast, for the trimer, we expect that this splitting is considerably reduced (due to the equivalent positions) but still present so that it may not be resolved. In analogy to the methanol trimer,[36] the remaining splitting is the result of the different orientations of the ethyl groups (methyl groups in the case of methanol) relative to the plane defined by the hydrogen-bonded OH groups. Consideration of the different conformers will result in additional splittings and/or broadening.

## Discussion

**Monomer.** The spectral region between 1020 and 1090 $cm^{-1}$ is difficult to analyze even for the ethanol monomer due to the strong coupling between the vibrational modes.[8,9] Shaw et al.[8] calculated geometries and relative energies of the *trans*- and *gauche*-conformers at the MP4 level. They determined harmonic frequencies but scaled the ab initio force field to improve the agreement with the experiment of Perchard and Josien.[9] Finally, they achieved excellent agreement with the experiment. Unfortunately, they fitted their synthetic spectrum to the spectrum measured for ethanol dissolved in $CS_2$ and not to the gas-phase ethanol spectrum. The problem is that, in the solution, the absorption lines are considerably broadened and shifted due

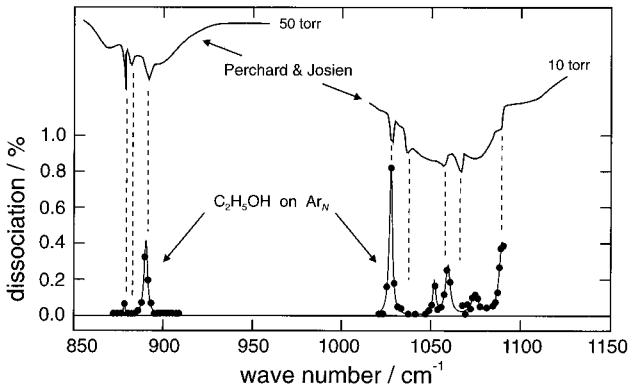


**Figure 10.** Overview spectrum of ethanol monomer adsorbed on argon clusters, containing both spectral regions studied, in comparison with the gas phase absorption spectrum adopted from Perchard and Josien.[9]

to the interaction with the solvent molecules. Furthermore, the solution spectrum may be governed by ethanol polymers, a conclusion which is supported by its close resemblance to the liquid-phase spectrum.[9] The same arguments apply to the theoretical study of Dothe et al.[10] since they also compared their results with the solution spectrum of Perchard and Josien.[9]

As far as the abundance of the two ethanol conformers (*trans* and *gauche*) is concerned, the theoretical studies favor the conclusion of Perchard and Josien[9] that the *gauche*-conformer predominates. This result, which is in contrast to the assertion of Barnes and Hallam,[11] is also supported by statistical arguments. While the energies of the two conformers are nearly degenerate, the statistical factor of 2 is in favor of the *gauche*-conformer because of the two possible orientations of the hydroxyl group. The *trans*−*gauche* separations of the vibrational bands calculated by Dothe et al.[10] are 4 $cm^{-1}$ for $\nu_s$(CCO), 23 $cm^{-1}$ for a doublet near 1030 $cm^{-1}$ ($\nu_\alpha$ in our notation), 6 $cm^{-1}$ for a doublet near 1060 $cm^{-1}$ ($\nu_\beta$), and finally 45 $cm^{-1}$ for the highest frequency vibration $\nu_\gamma$. Unfortunately, we do not know how much these separations are affected by the scaling procedure. Despite this uncertainty, we may conclude that some of the splittings observed in the spectrum of the ethanol monomer adsorbed on argon clusters might very well be explained by the existence of the two conformers. Thus, we assign the two lines in the $\nu_\beta$ band, which are separated by 7.6 $cm^{-1}$, to these two species. At the same time, we are tempted to attribute the weaker band at 1074.7 $cm^{-1}$ to the excitation of the $\nu_\gamma$ vibration in *trans*-ethanol while the *gauche*-conformer absorbs at 1089.3 $cm^{-1}$.

Following this interpretation, one would expect a similar splitting for the $\nu_\alpha$ line. In fact, it could very well be that another component of the $\nu_\alpha$ vibration is located below 1020 $cm^{-1}$, just outside the tuning range of the $CO_2$ laser. Strong support for this interpretation is provided by the observation of two lines in the gas phase[9] ($G_{1a}$ and $G_{1b}$) and in the argon matrix[11] ($M_{1a}$ and $M_{1b}$). As is demonstrated in Figure 6, this would further imply that the $\nu_\alpha$ band, observed for ethanol on argon clusters, corresponds to $G_{1b}$ in the gas phase and $M_{1b}$ in the matrix. Thus, we have the result that the $\nu_\alpha$ band (for ethanol on argon clusters) is red-shifted by 10.3 $cm^{-1}$ from the gas-phase line but slightly blue-shifted (by 2.3 $cm^{-1}$) from the matrix position. This observation is in accordance with the conception that the interaction with the chromophore is stronger in a rigid macroscopic matrix than in a more loosely bound argon cluster.

In Figure 10 we present a comparison between our monomer spectrum (obtained for ethanol on argon clusters) with the gas-phase data of Perchard and Josien.[9] The dashed vertical lines indicate the positions of the gas-phase Q-branches taken from

Table 1 of ref 9. Due to the one-to-one correspondence of most features, the agreement can be considered as very good. While in the region of the symmetric CCO stretch around 880 $cm^{-1}$ the present absorption lines are only slightly shifted to the red, the corresponding (red) shifts for the $\nu_\alpha$ and $\nu_\beta$ vibrations are between 6 and 10.3 $cm^{-1}$ (as has been discussed before). The highest frequency band $\nu_\gamma$ is observed at the same position in both studies. Note that the lower intensity band at 1047.7 $cm^{-1}$, which has been tentatively assigned to the $\nu_\gamma$ vibration of the *trans*-conformer, may be hidden in the gas-phase spectrum under the R-branch of the $\nu_\beta$ vibration.

In conclusion of the monomer discussion, we would like to give an explanation for the unexpected blue-shift of the two matrix lines denoted $M_{2a}$ and $M_{2b}$ in Figure 6. Besides the monomer lines discussed earlier, the matrix spectrum of Barnes and Hallam[11] shows some absorption bands that are attributed to ethanol polymers. We would arrive at a highly consistent picture if we assume that the two lines $M_{2a}$ and $M_{2b}$ are also polymeric lines and that, in contrast, the lines at 1051.9 and 1058 $cm^{-1}$, which are attributed to polymers (see the trimer spectrum of Figure 6), are the monomer lines expected around 1050 and 1058 $cm^{-1}$. Another even more plausible explanation would be that the matrix lines at 1051.9 and 1058 $cm^{-1}$ are to be attributed to polymers and that they mask the expected monomer lines.

**Dimer.** Now we would like to discuss the ethanol dimer spectra shown in Figures 5 and 6. The most prominent features of the spectrum obtained for $(C_2H_5OH)_2$ on $Ar_N$ are red-shifted by 1−2 $cm^{-1}$ from the gas-phase data. Besides that and the fact that the S/N ratio of the cluster-adsorbed spectrum is much better, the overall appearance is very similar. From our structure calculations we know that the ethanol dimer has an open-chain structure consisting of two nonequivalent monomer units. As a result, we expect each monomer line to split into two components which correspond to the excitation of the proton donor and acceptor, respectively. The situation should be the same as observed for the methanol dimer in both the C−O[1,5] and O−H[6] stretching regions. With this information it is quite logical to assign the two strong peaks observed at 1031.4 and 1045.4 $cm^{-1}$ in the gas phase [and at 1029.7 and 1043.9 $cm^{-1}$ for $(C_2H_5OH)_2$ attached to $Ar_N$] to the excitation of the $\nu_\alpha$ vibration in the nonequivalent constituents of the ethanol dimer. Without any further calculation it is difficult to decide which one of the two bands belongs to the proton acceptor and which to the proton donor. However, since we expect a larger shift for the proton donor, we tentatively assign the higher frequency component to this species.

As is indicated in Figure 6, the matrix study of Barnes and Hallam[11] shows two dimer peaks at 1027.5 and 1039.3 $cm^{-1}$ which are thus consistently red-shifted from our peaks. Unfortunately, the lower frequency dimer line observed in the matrix interferes with the monomer line $M_{1b}$ so that its actual position is not so clear. It should be emphasized that such accidental coincidence of monomer and dimer lines does not constitute a problem in the present study since a mass spectrometer is used to discriminate between the different contributions.

The interpretation of the other dimer features shown in Figure 6 is not so evident. Assuming that the two $\nu_\beta$ monomer lines (assigned to the *trans*- and *gauche*-conformers) further split in the dimer, and taking into account the possibility of different conformer combinations in the dimer, it would be conceivable that the two monomer lines merge into one broad dimer peak at 1060 $cm^{-1}$. Similarly, the structures beyond 1070 $cm^{-1}$ are attributed to $\nu_\gamma$ excitations in the various possible dimer constituents. As far as the symmetric CCO stretch is concerned, again a clear separation into two peaks is observed. According to the discussion presented before, they are assigned to the excitation of the symmetric CCO stretch in the proton acceptor and donor, respectively.

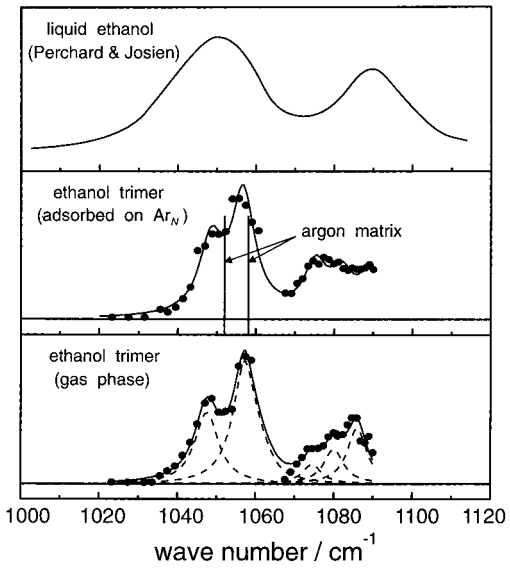


**Figure 11.** Comparison of the two trimer spectra (free gas phase and adsorbed on argon clusters) with the absorption spectrum measured by Perchard and Josien for liquid ethanol.[9]

**Trimer.** The trimer spectra shown in Figures 5 and 6 look much simpler than the respective dimer spectra. This can be rationalized with the help of our computational study. According to these calculations, the various possible ethanol trimers have cyclic structures with each constituent molecule playing the role of a proton donor *and* acceptor. For such structures we expect a considerable diminuation of the splittings encountered for the dimers. Such behavior has also been found for other hydrogen-bonded systems such as water and methanol.[1,5−7,16]

The two $\nu_\alpha$ dimer lines merge into one slightly broader band appearing at 1048 $cm^{-1}$. The $\nu_\beta$ vibration gives rise to a rather strong band at 1057 $cm^{-1}$. In contrast, the complicated structure of the $\nu_\gamma$ band seems to be preserved for the trimer. In the symmetric CCO stretching region at least three trimer lines are observed (see Figure 7). The interpretation of this structure is certainly complicated due to the existence of different conformers constituting the trimer.

Returning to the spectral region of the $\nu_\alpha$, $\nu_\beta$, and $\nu_\gamma$ vibrations, we would like to emphasize the similarity of the gas-phase and adsorbed trimer spectra. These two spectra are directly compared in Figure 11. In addition, we have included in this figure the liquid-phase ethanol spectrum measured by Perchard and Josien.[9] Although the liquid-phase absorptions are considerably broader, the similarity with the trimer spectra is indisputable. From this close resemblance one may conclude that, in the liquid, the ethanol molecules are arranged in cyclic structures consisting of three or perhaps more molecules. The latter conclusion assumes that the absorption spectra of the larger ethanol clusters ($n$ = 4, 5, ...) are not much different from the trimer spectrum. Exactly this observation was made for methanol clusters. Studying the C−O stretch of small methanol clusters, Buck and co-workers[2] found that the spectra for $n$ = 3, 4, and 5 were very similar and that a pronounced change only occurred for the hexamer.

## Conclusions

The present experiments on small ethanol complexes provide the first gas-phase study on this interesting system with size

selection. The rich structure of the dimer spectrum is explained with the existence of two nonequivalent molecules (proton donor and acceptor) in the hydrogen-bonded complex. The trimer spectrum is somewhat simpler, pointing to a cyclic structure of this complex. This interpretation is supported by calculations, yielding the minimum-energy configurations of ethanol dimers and trimers, and by comparing the experimental findings with the results of similar studies on methanol complexes.

Additional information is obtained for ethanol monomers, dimers, and trimers adsorbed on large argon host clusters. In contrast to conventional matrix isolation experiments, the molecular beam depletion technique, used in the present study, is able to identify the contribution of ethanol polymers since it combines IR absorption spectroscopy with mass spectrometric detection. In particular, it is shown that one may easily discriminate against the monomer if the absorption features of dimers and larger complexes are to be studied. The splittings observed in the absorption spectrum of ethanol molecules attached to argon host clusters are attributed to the existence of the two conformers, *trans*- and *gauche*-ethanol.

Although the tuning range of the $CO_2$ laser is very limited, we could investigate four vibrational modes, the in-plane and out-of-plane $CH_3$ rocking modes and the symmetric and asymmetric CCO stretches. The present study supplies high-quality spectra revealing the spectral evolution from the monomer to the liquid state. Due to the strong coupling between the vibrational motions and the fact that the ethanol molecule exists in two conformers, part of the interpretation of the spectral features must remain tentative. For a detailed analysis of the rich structure observed in the various spectra, new high-quality calculations should prove useful.

**Acknowledgment.** The authors like to thank Dr. B. Schmidt for fruitful discussions and for making his energy minimization program available. The continuous support of Professor H. Pauly is gratefully acknowledged. This work has been supported by the Deutsche Forschungsgemeinschaft (DFG).

## References and Notes

(1) Huisken, F.; Stemmler, M. *Chem. Phys. Lett.* **1988**, *144*, 391.
(2) Buck, U.; Gu, X. J.; Lauenstein, C.; Rudolph, A. *J. Chem. Phys.* **1990**, *92*, 6017.
(3) LaCosse, J. P.; Lisy, J. M. *J. Phys. Chem.* **1990**, *94*, 4398.
(4) Bizarri, A.; Stolte, S.; Reuss, J.; van Duijneveldt−van de Rijdt, J. G. C. M.; van Duijneveldt, F. B. *Chem. Phys.* **1990**, *143*, 423.
(5) Huisken, F.; Stemmler, M. *Z. Phys. D* **1992**, *24*, 277.
(6) Huisken, F.; Kulcke, A.; Laush, C.; Lisy, J. M. *J. Chem. Phys.* **1991**, *95*, 3924.
(7) Huisken, F.; Kaloudis, M.; Koch, M.; Werhahn, O. *J. Chem. Phys.* **1996**, *105*, 8965.
(8) Shaw, A.; Wieser, H.; Dutler, R.; Rauk, A. *J. Am. Chem. Soc.* **1990**, *112*, 5401.
(9) Perchard, J.-P.; Josien, M.-L. *J. Chim. Phys. Physicochim. Biol.* **1968**, *65*, 1834, 1856.
(10) Dothe, H.; Lowe, M. A.; Alper, J. S. *J. Chem. Phys.* **1989**, *93*, 6632.
(11) Barnes, A. J.; Hallam, H. E. *Trans. Faraday Soc.* **1970**, *66*, 1932.
(12) Crooks, J.; Stace, A. J.; Whitaker, B. J. *J. Phys. Chem.* **1988**, *92*, 3554.
(13) Buck, U.; Meyer, H. *Phys. Rev. Lett.* **1984**, *52*, 109.
(14) Huisken, F.; Pertsch, T. *Chem. Phys.* **1988**, *126*, 213.
(15) Huisken, F.; Kaloudis, M.; Kulcke, A.; Laush, C.; Lisy, J. M. *J. Chem. Phys.* **1995**, *103*, 5366.
(16) Huisken, F.; Kaloudis, M.; Kulcke, A. *J. Chem. Phys.* **1996**, *104*, 17.
(17) Huisken, F.; Kaloudis, M.; Koch, M. *J. Chem. Phys.*, to be published.
(18) Gough, T. E.; Mengel, M.; Rowntree, P. A.; Scoles, G. *J. Chem. Phys.* **1985**, *83*, 4958.
(19) Huisken, F.; Stemmler, M. *J. Chem. Phys.* **1993**, *98*, 7680.
(20) Ehbrecht, M.; de Meijere, A.; Stemmler, M.; Huisken, F. *J. Chem. Phys.* **1992**, *97*, 3021.
(21) Rohmund, F.; Huisken, F. *J. Chem. Phys.* **1997**, *107*, 1045.
(22) Huisken, F. *Adv. Chem. Phys.* **1992**, *81*, 63.
(23) Mori, Y.; Kitagawa, T. *Chem. Phys. Lett.* **1986**, *128*, 383.
(24) Morgan, S.; Castleman, Jr., A. W. *J. Phys. Chem.* **1989**, *93*, 4544.
(25) Ehbrecht, M.; Stemmler, M.; Huisken, F. *Int. J. Mass Spectrom. Ion Processes* **1993**, *123*, R1.
(26) Fröchtenicht, R.; Kaloudis, M.; Koch, M.; Huisken, F. *J. Chem. Phys.* **1996**, *105*, 6128.
(27) Buck, U.; Schmidt, B. *J. Chem. Phys.* **1993**, *98*, 9410.
(28) Press, W. H.; Flannery, B. P.; Teukolsky, S. A.; Vetterling, W. T. *Numerical Recipes*; Cambridge University: Cambridge, 1989.
(29) Alagona, G.; Tani, A. *J. Chem. Phys.* **1981**, *74*, 3980.
(30) Jorgensen, W. L. *J. Phys. Chem.* **1986**, *90*, 1276.
(31) Bleiber, A.; Sauer, J. *Chem. Phys. Lett.* **1995**, *238*, 243.
(32) van Duijneveldt−van de Rijdt, J. G. C. M.; van Duijneveldt, F. B. *Chem. Phys.* **1993**, *175*, 271.
(33) Xantheas, S. S.; Dunning, Jr., T. H. *J. Chem. Phys.* **1993**, *98*, 8037.
(34) Klopper, W.; Schütz, M. *Ber. Bunsen-Ges. Phys. Chem.* **1995**, *99*, 469.
(35) González, L.; Mó, O.; Yáñez, M.; Elguero, J. *J. Mol. Struct. (THEOCHEM)* **1996**, *371*, 1.
(36) Mó, O.; Yáñez, M.; Elguero, J. *J. Mol. Struct. (THEOCHEM)* **1994**, *314*, 73.